Farese, R. V., Sabir, M. A., & Larson, R. E. (1980c) *Proc. Natl. Acad. Sci. U.S.A. 77*, 7189.
Farese, R. V., Larson, R. E., & Sabir, M. A. (1980d) *Biochim. Biophys. Acta 633*, 479.
Farese, R. V., Bidot-Lopez, P., Sabir, M. A., Smith, J., Schinbeckler, B., & Larson, R. (1980e) *J. Clin. Invest. 65*, 1523.
Farese, R. V., Sabir, M. A., & Larson, R. E. (1980f) *J. Clin. Invest. 66*, 1428.
Ferguson, J. J., Jr. (1963) *J. Biol. Chem. 238*, 2754.
Garren, L. E., Ney, R. L., & Davis, W. W. (1965) *Proc. Natl. Acad. Sci. U.S.A. 53*, 1443.
Haynes, R. C., & Berthet, L. (1957) *J. Biol. Chem. 225*, 115.
Hokin, L. E., & Hokin, M. R. (1958) *J. Biol. Chem. 233*, 805.
Hokin, M. R., & Hokin, L. E. (1959) *J. Biol. Chem. 234*, 1381.
Hosaka, K., Yamashita, S., & Numa, S. (1975) *J. Biochem. (Tokyo) 77*, 501.
Kabara, J. J., & Chen, J. S. (1976) *Anal. Chem. 48*, 814.
Lamb, R. E., & Fallon, H. J. (1970) *J. Biol. Chem. 254*, 3075.
Lowry, O. H., Rosebrough, N. J., Farr, A. L., & Randall, J. (1951) *J. Biol. Chem. 193*, 265.
Martensson, E., & Kanfer, J. (1968) *J. Biol. Chem. 243*, 497.
Merlie, J. P., & Pizer, L. I. (1973) *J. Bacteriol. 116*, 355.
Michell, R. H. (1975) *Biochim. Biophys. Acta 414*, 81.
Silber, R. H., Busch, R., & Oslapas, R. (1958) *Clin. Chem. (Winston-Salem, N.C.) 4*, 278.

Divalent Metal Ion, Inorganic Phosphate, and Inorganic Phosphate Analogue Binding to Yeast Inorganic Pyrophosphatase†

Barry S. Cooperman,* Anna Panackal, Bleecker Springs, and Donald J. Hamm‡

ABSTRACT: Four different techniques, equilibrium dialysis, protection of enzymatic activity against chemical inactivation, ^{31}P relaxation rates, and water proton relaxation rates, are used to study divalent metal ion, inorganic phosphate, and inorganic phosphate analogue binding to yeast inorganic pyrophosphatase, EC 3.6.1.1. A major new finding is that the binding of a third divalent metal ion per subunit, which has elsewhere been implicated as being necessary for enzymatic activity [Springs, B., Welsh, K. M., & Cooperman, B. S. (1981) *Biochemistry* (in press)], only becomes evident in the presence of added inorganic phosphate and that, reciprocally, inorganic phosphate binding to both its high- and low-affinity sites on the enzyme is markedly enhanced in the presence of divalent metal ions, with Mn^{2+} causing an especially large increase in affinity. The results obtained allow evaluation of all of the relevant equilibrium constants for the binding of Mn^{2+} and inorganic phosphate or of Co^{2+} and inorganic phosphate to the enzyme and show that the high-affinity site has greater specificity for inorganic phosphate than the low-affinity site. In addition, they provide evidence against divalent metal ion inner sphere binding to phosphate for enzyme subunits having one or two divalent metal ions bound per subunit and evidence for a conformational change restricting active-site accessibility to solvent on the binding of a third divalent metal ion per subunit.

Work in this laboratory over the last few years has been devoted to elucidating the mechanism of action of the dimeric enzyme yeast inorganic pyrophosphatase, EC 3.6.1.1 (PPase).[1] This enzyme catalyzes both pyrophosphate (PP_i) hydrolysis and water–phosphate (P_i) oxygen exchange. In recent papers (Hamm & Cooperman, 1978; Springs et al., 1981) we have presented a unified scheme for PPase action which accounts quantitatively for the observed overall rate constants for both processes and, in addition, presented evidence that three Mg^{2+} per active subunit are required for enzymatic activity and that there are two P_i sites per subunit, one of high and one of low affinity. We will henceforth denote these sites as site 1 and site 2, respectively.

Although Mg^{2+} confers maximal activity on PPase, appreciable activity is also found in the presence of Zn^{2+}, Co^{2+}, and Mn^{2+} (Butler & Sperow, 1977; Janson et al., 1979). In this paper we use four different techniques, equilibrium dialysis, protection of enzymatic activity against chemical modification, ^{31}P relaxation rates, and water proton relaxation rates, to investigate divalent metal ion, P_i, and P_i analogue (methylphosphonate, thiophosphate, and phosphoramidate) binding to PPase. The binding of P_i in the presence of either Mn^{2+} or Co^{2+} has been investigated in the most detail, because the paramagnetism of these two metal ions will make them extremely useful in future NMR and ESR studies.

Our major findings and conclusions are as follows. (1) In addition to the two divalent metal ions bound with approximately equal affinity per PPase subunit in the absence of P_i, a third divalent metal ion is bound with approximately equal affinity in the presence of P_i. (2) Reciprocally, the affinity of P_i for both of its sites on PPase is markedly increased in the presence of divalent metal ion. In the presence of either Mn^{2+} or Co^{2+}, the binding to site 1 is strong enough to permit direct stoichiometric titration. (3) The equilibrium dialysis and ^{31}P relaxation rate studies permit evaluation of all of the relevant equilibrium constants for the binding of three Mn^{2+}

† From the Department of Chemistry, University of Pennsylvania, Philadelphia, Pennsylvania 19104. *Received April 16, 1981.* This work was supported by a research grant from the National Institutes of Health (AM-13212).
‡ Present address: Best Food, a unit of CPC International, Union, NJ 07083.

[1] Abbreviations used: BSA, bovine serum albumin; PEI, poly(ethylenimine); EDAC, 1-ethyl-3-[3-(dimethylamino)propyl]carbodiimide; PhGx, phenylglyoxal; P_i, inorganic phosphate; PP_i, inorganic pyrophosphate; PPase, yeast inorganic pyrophosphatase; PRR, proton relaxation rate; Cl_3CCOOH, trichloroacetic acid; Tris, tris(hydroxymethyl)-aminomethane.

0006-2960/81/0420-6051$01.25/0

ions and two phosphates or three Co^{2+} ions and two phosphates to PPase. (4) The structural specificity of site 1 for P_i is greater than that of site 2. (5) Several lines of evidence support the suggestion that the binding of a third divalent metal ion is accompanied by a conformational change of the enzyme which has the effect of reducing solvent accessibility to the active site. (6) In enzyme subunits having one or two divalent metal ions bound per subunit, our evidence indicates an absence of divalent metal ion inner sphere binding to P_i in either site 1 or site 2.

Experimental Procedures

Materials

PPase was prepared with some minor modifications (Bond, 1979) of the procedure described previously and had a specific activity of 550–750 IU/mg as measured by the standard titrimetric assay (Cooperman et al., 1973). Trisodium thiophosphate was prepared according to Åkerfeldt (1960) and was contaminated with 1–2% P_i as estimated by ^{31}P NMR. Methylphosphonic acid was a gift from A. Hampton (Institute for Cancer Research, Fox Chase, PA). Monopotassium phosphoramidate was prepared according to Klement & Becht (1947) as modified by Chambers & Khorana (1958). This material as prepared was free of P_i. However, prolonged standing in solution at pH 7 did lead to hydrolysis. For example, samples stored overnight at 4 °C were 2–4% in P_i. Phenylglyoxal (PhGx) was obtained from Aldrich Chemical Co. and 1-ethyl-3-[3-(dimethylamino)propyl]carbodiimide (EDAC) from Sigma Chemical Co. Carrier-free [^{32}P]P_i was from ICN, and carrier-free $^{54}Mn^{2+}$ and $^{57}Co^{2+}$ were from New England Nuclear. *N*-Ethylmorpholine (Pierce, Sequanal Grade) was distilled before use. Dialysis tubing (3787-D52, 12000 molecular weight cutoff) was obtained from A. H. Thomas and prewashed by boiling with distilled water and rinsing with distilled deionized water. Water for stock solutions was glass distilled and passed through a Barnstead standard mixed-bed deionized column. Stock solutions of Tris (Trizma, Sigma) and KCl used for making up buffers for both the dialysis and NMR experiments were passed over Chelex 100 (Bio-Rad) to reduce trace heavy metal ion contamination. Stock solutions of divalent metal ion salts were prepared by weight from analytical grade samples. Solutions of $MnCl_2 \cdot 4H_2O$ were standardized by using Eriochrome Black T (West, 1969).

Methods

Equilibrium Dialysis. All dialysis experiments were carried out in buffer A [0.10 M Tris-HCl (pH 7.2, measured at room temperature) and 0.10 M KCl]. Two methods were employed. Data obtained with method A were used in construction of the Scatchard plots shown in Figures 1 and 2. In this method samples were placed in a Technilab multicavity microdialysis cell (Bel-Art Products) in which each cavity had a volume of 100 μL. In all cases radioactive ligand and enzyme were added to cavities on opposite sides of the dialysis membrane at the beginning of the experiment. The dialysis cells were gently rotated overnight at room temperature (21–23 °C) on a Technilab rotator (Model 71-Bel Art Products), which suitable control experiments showed to be sufficient for the attainment of equilibrium. Following the attainment of equilibrium, aliquots were taken to determine the concentration of radioactive ligand in both cavities and the concentration of enzyme on the enzyme side (this was necessary because the enzyme concentration typically changed during the course of a dialysis experiment). Concentrations of $^{54}Mn^{2+}$ and $^{57}Co^{2+}$ were determined by using a well γ counter coupled to a Northern NS 600 multichannel analyzer. Concentrations of [^{32}P]P_i were determined by using a liquid scintillation counter as described elsewhere (Springs et al., 1981). Concentrations of PPase were determined by using the protein determination technique of Schaffner & Weissman (1973). Method B was used to prepare samples for ^{31}P NMR measurements, as described previously (Hamm & Cooperman, 1978).

Enzyme Inactivation. Rates of PPase inactivation by PhGx or EDAC were determined as previously described (Cooperman & Chiu, 1973b; Bond et al., 1980). All inactivations were carried out in buffer B [0.12 ± 0.02 M *N*-ethylmorpholine acetate (pH 7.0, measured at room temperature)] at 25.0 °C. PhGx concentration varied from 10 to 50 mM. EDAC concentration was always 50 mM.

Nuclear Relaxation Rates. The longitudinal proton relaxation rate (PRR) of water ($1/T_1$) was measured at 24.3 MHz by a pulsed nuclear magnetic resonance technique described previously (Cohn & Leigh, 1962). Values of the observed enhancements (Eisinger et al., 1962), ϵ_{obsd}, were calculated from

$$\epsilon_{obsd} = \frac{1/T_1^* - 1/T_{1,0}^*}{1/T_1 - 1/T_{1,0}} \quad (1)$$

where $1/T_1$ and $1/T_{1,0}$ are the observed relaxation rates in the presence and absence of Mn^{2+}, respectively. The terms with astericks represent the same rates measured in the presence of inorganic pyrophosphatase. In the absence of enzyme, added P_i has essentially no effect on either $1/T_1$ or $1/T_{1,0}$. Sample volumes varied from 50 to 100 μL.

The longitudinal phosphorus nuclear magnetic relaxation rates of P_i ($1/T_1^P$) and of P_i analogues were measured at 40.3 MHz by Fourier transform NMR as described earlier (Hamm & Cooperman, 1978). All NMR experiments were conducted at 25 ± 2 °C in buffer A.

Enzyme concentration was measured spectrophotometrically by using an extinction coefficient of 1.45 at 280 nm (Kunitz, 1952) for a 0.1% solution of inorganic pyrophosphatase and a subunit weight of 35000 (Cooperman & Chiu, 1973a; Bond et al., 1980).

Results

We have investigated the binding to PPase of divalent metal ions, P_i, and P_i analogues by four different techniques: equilibrium dialysis, protection of enzyme activity against chemical modification, ^{31}P NMR, and water proton relaxation rates. The results of these studies are presented in turn below. Parameters used in equations are defined either in Table I, in Table VIII, or in the text.

Equilibrium Dialysis. The binding of $^{54}Mn^{2+}$ and $^{57}Co^{2+}$ to enzyme in the presence and absence of added P_i was measured by equilibrium dialysis, and the results, plotted in Scatchard form (Scatchard, 1949), are presented in Figure 1. In agreement with the work of Rapoport et al. (1973), we find a stoichiometry of two tightly bound metal ions per subunit for both Mn^{2+} and Co^{2+}. A new result of our work is the demonstration that in the presence of sufficient P_i, three metal ions are tightly bound per subunit. Because of the considerable scatter in most of our data, we have chosen to interpret our results in the simplest possible way, as in each case reflecting binding to intrinsically equal affinity sites. Accordingly, the lines drawn in Figure 1 are linear least-squares fits to

$$\frac{\nu}{[M^{2+}]} = \frac{[n - \nu]}{K} \quad (2)$$

Table I: Parameter Definitions

Conservation and Apparent Equilibrium Constants	
$[E]_T$, $[M^{2+}]_T$, $[P]_T$	total concentration in all their forms of enzyme, divalent metal ion, and P_i or P_i analogue, respectively; specific terms, such as $[Mn^{2+}]_T$ or $[P_i]_T$ are also used
$[M^{2+}]_B$	total concentration of divalent metal ion bound to enzyme
$K_{p,app}$, $K_{p_1,app}$, $K_{p_2,app}$	apparent dissociation constants for P_i or P_i analogue binding to enzyme; subscripts 1 and 2 refer to high- and low-affinity P_i site binding, respectively
Protection against Inactivation	
k_o	second-order rate constant for inactivation in the absence of added P_i or P_i analogue
k_s	second-order rate constant for inactivation in the presence of divalent metal ion and saturating P_i or P_i analogue
^{31}P NMR	
T_{ip}^P	paramagnetic contribution to $T_{i,obsd}^P$
T_{ib}^P	T_1 in the binary CoP_i complex
T_{ic}^P	contribution of enzyme-bound paramagnetic ion to T_{ip}^P
T_{iq}^P	T_1 in the complex EMP_2, where M is Mn^{2+} or Co^{2+}
$T_{iq'}^P$	T_1 in the complex EM_2P_2, where M is Mn^{2+} or Co^{2+}
Water Proton Relaxation Rates	
ϵ_b	enhancement of the EMn complex
ϵ_t	enhancement of the EMnP complex
ϵ_q	enhancement of the $EMnP_2$ complex
$\epsilon_{t'}$	enhancement per Mn^{2+} in the EMn_2P complex
$\epsilon_{q'}$	enhancement per Mn^{2+} in the EMn_2P_2 complex
ϵ_s	limit of ϵ_{obsd} at saturating $[P]_T$

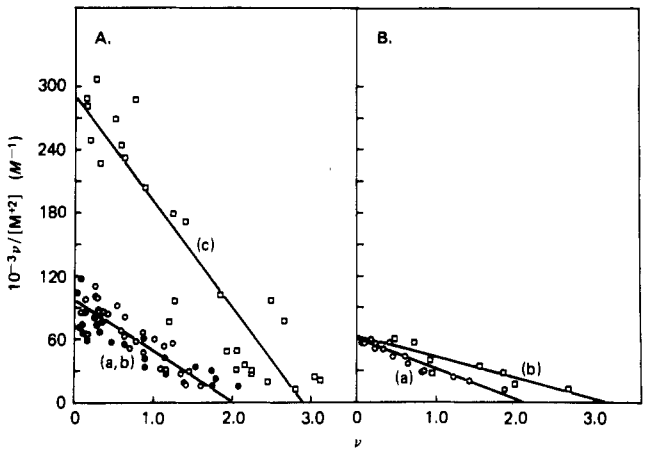

FIGURE 1: Scatchard plots of metal ion binding to PPase as measured by equilibrium dialysis. (A) Mn^{2+} binding: (a) no added P_i, enzyme concentration 7–42 μM (○); (b) in the presence of 50 μM P_i, enzyme concentration 7–36 μM (●); (c) in the presence of 4 mM P_i, enzyme concentration 8–116 μM (□). (B) Co^{2+} binding: (a) no added P_i, enzyme concentration 8–96 μM (○); (b) in the presence of 2.5 mM P_i, enzyme concentration 30–35 μM (□).

where ν is the number of divalent metal ions bound per enzyme subunit, n is the number of divalent metal ions bound at saturation, and K is the intrinsic dissociation constant. The apparent dissociation constants for the binding of the first, second, and, where appropriate, third metal ions per subunit, which are related to the intrinsic binding constant by purely statistical corrections, are listed in Table II, as are the extrapolated values of n.

The binding of P_i to enzyme in the presence of Mn^{2+} and Co^{2+} was also measured by equilibrium dialysis. Scatchard analysis (Figure 2), the results of which are summarized in Table II, clearly shows the presence of one high-affinity site per subunit. In the absence of divalent metal ions, P_i binding to PPase is weak, with preliminary studies indicating a lower limit of 0.5 mM for the dissociation constant (data not shown).

Table II: Apparent Dissociation Constants and Binding Stoichiometries As Determined by Equilibrium Dialysis

varying ligand	[fixed ligand] (mM)	$K_{1,app}$ (mM)	$K_{2,app}$ (mM)	$K_{3,app}$ (mM)	n
Mn^{2+}		0.0103	0.041		2.0
Mn^{2+}	P_i, 0.05	0.0103	0.041		2.0
Mn^{2+}	P_i, 4.0	0.00347	0.0104	0.0312	2.9
Co^{2+}		0.0165	0.066		2.1
Co^{2+}	P_i, 2.5	0.0158	0.048	0.143	3.2
P_i	Mn^{2+}, 0.5	0.0137			1.05
P_i	Co^{2+}, 1.0	0.056			0.85

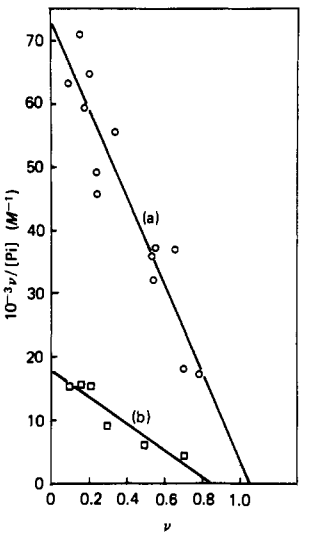

FIGURE 2: Scatchard plots of P_i binding to PPase as measured by equilibrium dialysis. (a) In the presence of 0.5 mM Mn^{2+}, enzyme concentration 22–36 μM (○); (b) in the presence of 1.0 mM Co^{2+}, enzyme concentration 21–113 μM (□).

Protection of Enzymatic Activity against Chemical Modification. We have previously shown that PPase is inactivated by PhGx and that although Mn^{2+} or Ca^{2+} alone does not protect against such inactivation, the combination of either Mn^{2+} and the competitive inhibitor hydroxymethanediphosphonate or Ca^{2+} and PP_i afford strong protection (Cooperman & Chiu, 1973b; Bond et al., 1980). This approach has now been extended to examine whether P_i and methylphosphonate protect the enzyme from PhGx inactivation. Under pseudo-first-order conditions (excess PhGx), second-order rate constants (k_{obsd}) were determined for PhGx inactivation of PPase at fixed metal ion concentration and varying P_i or methylphosphonate concentrations. The results obtained, when plotted in double-reciprocal fashion according to eq 3 (Figure 3), yield apparent dissociation constants, $K_{p,app}$, for P_i and methylphosphonate

$$\frac{1}{1-a} = \frac{1}{1-b} + \frac{1}{1-b}\frac{K_{p,app}}{[P]} \qquad (3)$$

where [P] is equal to the P_i or methylphosphonate concentration, a is equal to k_{obsd}/k_0, b is equal to k_s/k_0, and k_0 and k_s are the second-order rate constants for inactivation of the enzyme in the absence of P_i or methylphosphonate and in the presence of saturating P_i or methylphosphonate, respectively.[2]

[2] We interpret the dependence of the rate of PhGx inactivation of enzyme as a function of P_i concentration as reflecting a single P_i binding process (Figure 3). This procedure is necessary because our data are insufficiently precise to justify an attempt to define two binding processes but will yield a $K_{p,app}$ intermediate between $K_{p1,app}$ and $K_{p2,app}$ if the binding of the first P_i confers only partial protection.

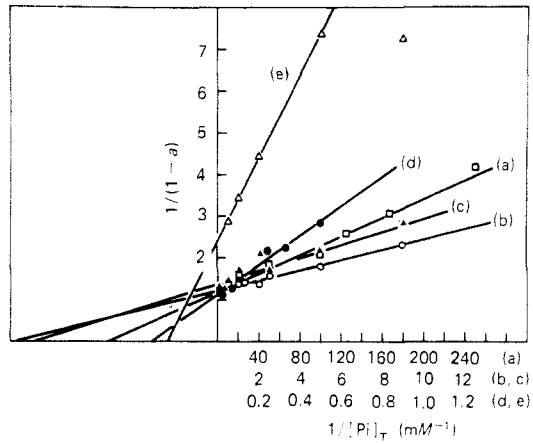

FIGURE 3: Rates of phenylglyoxal inactivation of PPase, plotted according to eq 3. (a) In the presence of Mn^{2+} and varying P_i (□); (b) in the presence of Co^{2+} and varying P_i (○); (c) in the presence of Zn^{2+} and varying P_i (▲); (d) in the presence of Mg^{2+} and varying P_i (●); (e) in the presence of Mn^{2+} and varying methylphosphonate (△).

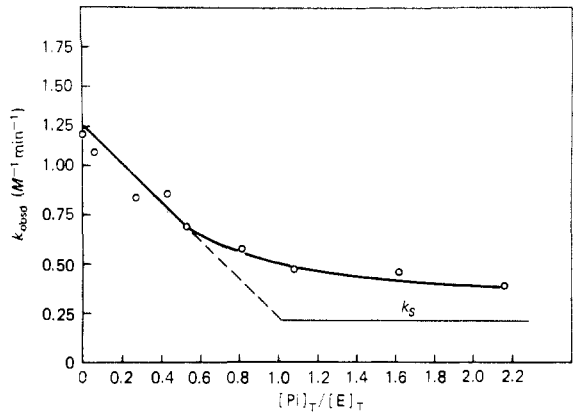

FIGURE 4: Rate of PhGx inactivation of PPase as a function of $[P_i]_T/[E]_T$. $[E]_T$, 0.37 mM; $[Mn^{2+}]_T$, 4.0 mM.

Table III: Studies on Protection against Chemical Inactivation

$[E]_T$ (mM)	[fixed ligand] (mM)	varying ligand	reagent	k_0 (M^{-1} min^{-1})	k_s (M^{-1} min^{-1})	$K_{p,app}$ (mM)
0.0023	Mn^{2+}, 1.0	P_i	PhGx	1.15	0.21	0.0094
0.028	Co^{2+}, 1.0	P_i	PhGx	1.28	0.23	0.090
0.028	Mg^{2+}, 10	P_i	PhGx	1.29	0.31	2.4
0.028	Zn^{2+}, 1.0	P_i	PhGx	1.08	0.31	0.111
0.028	Mn^{2+}, 1.0	CP[a]	PhGx	1.15	0.68	4.1
0.027	P_i, 3.0		PhGx	0.60		
0.033	Mn^{2+}, 0.4		EDAC	0.92		
0.0095	Co^{2+}, 1.0	P_i	EDAC	2.54	0.68	0.058
0.025	Mg^{2+}, 10	P_i	EDAC	2.58	0.20	4.5
0.030	Zn^{2+}, 0.9	P_i	EDAC	1.78	0.35	0.18

[a] Methylphosphonate.

$K_{p,app}$, k_0, and k_s values are listed in Table III. As expected, k_0 values are almost independent of the identity of added divalent metal ions, reflecting the lack of protection offered by metal ions alone. By contrast, added P_i alone (3 mM) affords significant protection, providing evidence that P_i binds to enzyme even in the absence of added metal ion.

In the presence of Mn^{2+} protection by P_i is exerted at especially low P_i concentration, and, accordingly, the Mn^{2+}–P_i system was investigated further. A plot of k_{obsd} vs. $[P_i]_T/[E]_T$ at fixed $[Mn^{2+}]_T$ and an enzyme concentration (0.37 mM in subunits) large compared to $K_{p,app}$ is presented in Figure 4. The stoichiometry of P_i binding per subunit necessary for protection can be estimated as being equal to 1.01, measured

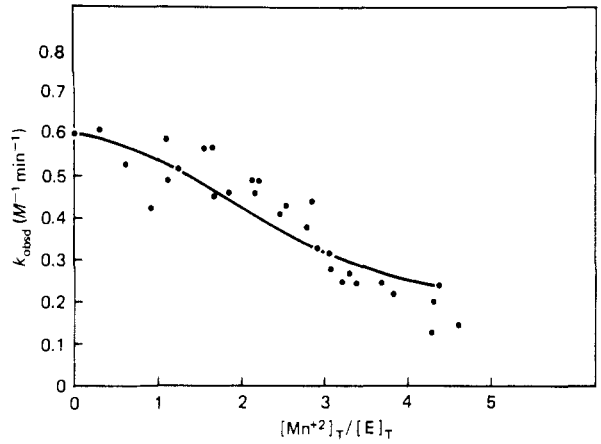

FIGURE 5: Rate of PhGx inactivation of PPase as a function of $[Mn^{2+}]_T/[E]_T$. The total concentrations of enzyme and P_i were fixed at 0.025 mM and 3.0 mM, respectively. The line drawn is theoretical (see text).

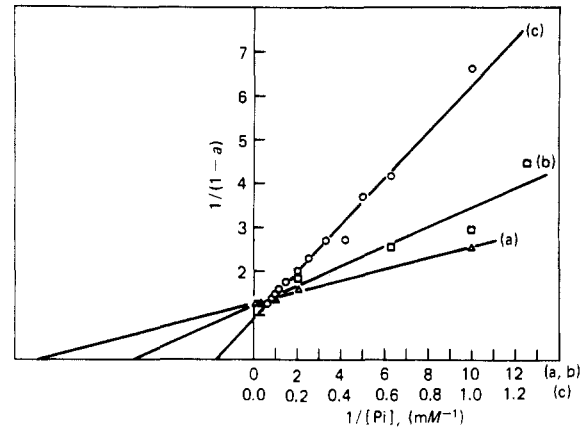

FIGURE 6: Rates of EDAC inactivation of PPase, plotted according to eq 3. (a) In the presence of Co^{2+} and varying P_i (△); (b) in the presence of Zn^{2+} and varying P_i (□); (c) in the presence of Mg^{2+} and varying P_i (○).

as the point of intersection of the initial slope and the line corresponding to k_s (see Table III).

The rate of PhGx inactivation of PPase was also studied at fixed P_i concentration and varying Mn^{2+}/enzyme ratios, as shown in Figure 5. The results clearly indicate that full protection requires, in addition to P_i, more than one bound Mn^{2+}/enzyme. Below we will show the data presented under Results permit estimation of all of the relevant constants describing Mn^{2+} and P_i binding to enzyme (see Table VIII). These estimates, in turn, permit calculation of the concentration of various enzyme species at given $[E]_T$, $[Mn^{2+}]_T$, and $[P_i]_T$. In the presence of 3 mM P_i, the dominant enzyme species in solution during the course of the titration with Mn^{2+} are EP_i, $EMnP_i$, $EMn_2(P_i)_2$, and $EMn_3(P_i)_2$. The initial and plateau values of k_{obsd} provide estimates of the second-order rate constants for EP_i and $EMn_3(P_i)_2$, which are 0.60 and 0.12 M^{-1} min^{-1}, respectively. A simple curve-fitting procedure allows estimation of rate constants of 0.60 and 0.38 M^{-1} min^{-1} for $EMnP_i$ and $EMn_2(P_i)_2$, respectively. The line in Figure 5 is drawn by using these estimates. These results show that maximal protection requires, in addition to the binding of P_i, the binding of three Mn^{2+} per subunit. Second-order rate constants for enzyme inactivation were also obtained in the presence of excess EDAC, fixed metal ion concentration, and varying P_i concentration (Figure 6) and analyzed as described above for the PhGx studies, with the results summarized in Table III.

Table IV: ^{31}P Longitudinal Rate Studies

$[E]_T$ (mM)	[fixed ligand] (mM)	variable ligand	$K_{p,app}$ (mM)	$1/T^p_{1,complex}$ (s^{-1})	ref
	Co^{2+}, 0.05	P_i	4.6	$1/T_{1b}$, 3.6×10^2	*a*
0.94	Co^{2+}, 0.50	P_i	11.5	$1/T_{1q}$, 1.1×10^2	*a*
1.00	Co^{2+}, 1.8	P_i	3.8	$1/T_{1q'}$, 2.7×10^2	*a*
0.10	Mn^{2+}, 0.040	SP[c]	136	$1/T_{1q}$, 5.1×10^3	*a*
0.10	Mn^{2+}, 0.040	CP[d]	6.7		*a*
			35	$1/T_{1q}$, 2.3×10^3	*a*
0.10	Mn^{2+}, 0.015	P_i	18	$1/T_{1q}$, 4.4×10^3	*b*

[a] This work (Figure 7). [b] Hamm & Cooperman, 1978. [c] Thiophosphate. [d] Methylphosphonate.

Table V: Evaluation of T^p_{1c} by the Dialysis Method

$[E]_T$ (mM)	$[Co^{2+}]_T$ (mM)	$[P_i]_T$ (mM)	$T^p_{1,obsd}$ (enzyme side)	$T^p_{1,obsd}$ (nonenzyme side)	T^p_{1c}
1.0	1.8	5.0	0.033 ± 0.003	1.5 ± 0.25	0.034
1.0	1.8	50	0.20 ± 0.020	1.8 ± 0.1	0.232

^{31}P Longitudinal Relaxation Rates. We previously showed that T^p_{1p}, the paramagnetic contribution to $T^p_{1,obsd}$, could be used to measure the interaction of EMn with P_i in solutions of enzyme, Mn^{2+}, and P_i (Hamm & Cooperman, 1978). This approach is now extended to study P_i interactions with ECo. We first determined the relaxation time T^p_{1b} and the dissociation constant K_B for the binary CoPi complex. At constant $[Co^{2+}]_T$ (0.050 mM), T^p_{1p} varied linearly as a function of added P_i (10–40 mM), permitting calculation of T^p_{1b} and K_B according to eq 4 (Navon et al., 1970) (see Table IV)

$$[Co^{2+}]_T T^p_{1p} = T^p_{1b}(K_B + [P_i]) \quad (4)$$

In our previous work we found that the binding of P_i to the high-affinity site (site 1) of EMn made no apparent contribution to T^p_{1p} so that such measurements could be used to calculate $K_{p_2,app}$ and T^p_{1q} according to eq 5, where $K_{p_2,app}$ reflects

$$[M^{2+}]_B T^p_{1c} = T^p_{1q}(K_{p_2,app} + [P]) \quad (5)$$

binding to the low-affinity site (site 2), T^p_{1c} is the contribution of enzyme-bound paramagnetic ion to T^p_{1p}, T^p_{1q} is the relaxation time in the complex EMP_2, and $[M^{2+}]_B$ is the total concentration of divalent metal ion bound to enzyme. As seen in Figure 7, T^p_{1c} is also a linear function of added P_i in solutions of enzyme and Co^{2+}. The slope and intercept of line a allow calculation of $K_{p_2,app}$ and T^p_{1q} for $ECoP_2$, and these values in turn permit calculation of $K_{p_2,app}$ and $T^p_{1q'}$ from the slope and intercept of line b, where $T^p_{1q'}$ is the relaxation time in the complex ECo_2P_2. These values are collected in Table IV.

T^p_{1p} values have also been measured to study P_i analogue binding to EMn. The linear behavior seen as a function of thiophosphate concentration (Figure 7, line c) allows calculation of $K_{p,app}$ and T^p_{1q} values for this analogue. T^p_{1q} is similar to what was found previously for P_i, which may be taken as evidence that thiophosphate binds to site 2 with the same orientation relative to Mn^{2+} as does P_i, but the affinity of thiophosphate for the enzyme is ~9-fold less compared to that of P_i (Table IV). In the case of methylphosphonate, a more complex curve is observed (Figure 7, line d). A simple model consistent with the observed concentration dependence of T^p_{1p} involves obligatory ordered binding of methylphosphonate to site 1 prior to binding to site 2, with only site 2 binding contributing to T^p_{1p}. This model is described by

$$[M^{2+}]_B T^p_{1c} = T^p_{1q} \frac{(K_{p_1,app}K_{p_2,app} + [P]K_{p_2,app} + [P]^2)}{[P]} \quad (6)$$

where $K_{p_1,app}$ and $K_{p_2,app}$ are the dissociation constants for high affinity site and low affinity site binding, respectively. It should be noted that if $K_{p_1,app} \ll [P]$, which is the situation for P_i binding to enzyme–Mn^{2+} and enzyme–Co^{2+} over the entire accessible concentration range (see discussion below), then eq 6 reduces to eq 5. Values of $K_{p_1,app}$, $K_{p_2,app}$, and T^p_{1q} were obtained by fitting the data in curve c to eq 6, using a computerized nonlinear least-squares fitting procedure (Lietzke, 1963). The average values from two such experiments are listed in Table IV.

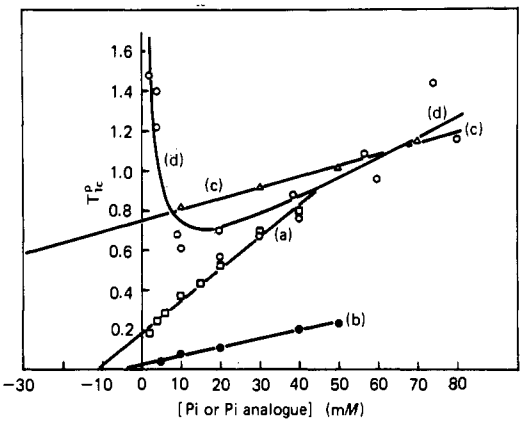

FIGURE 7: Dependence of T^p_{1c} on P_i or P_i analogue concentration. (a) $[E]_T$, 0.94 mM, Co^{2+}, 0.50 mM, and varying P_i (□); (b) $[E]_T$, 1.0 mM, Co^{2+}, 1.8 mM, and varying P_i (●); (c) $[E]_T$, 0.10 mM, Mn^{2+}, 0.04 mM, and varying thiophosphate (△); (d) $[E]_T$, 0.10 mM, Mn^{2+}, 0.04 mM, and varying methylphosphonate (○). Lines a–c are linear least-squares fits to the results. Line d is a nonlinear least-square fit (see text).

Equations 5 and 6 require determination of $[Mn^{2+}]_B$ and T^p_{1c} in order to evaluate T^p_{1q} and the apparent dissociation constants. For curve b in Figure 7, in which the $[Co^{2+}]_T$/[enzyme]$_T$ ratio is 1.8:1.0, T^p_{1c} was determined at two different P_i concentrations, 5 and 50 mM, as shown in Table V. On the basis of these results, small corrections were applied to the rest of the measured T^p_{1p} values to give estimated T^p_{1c} values, and $[Co^{2+}]_B$ was approximated by $[Co^{2+}]_T$. For the remainder of the curves in Figure 7, [enzyme]$_T$, $[Co^{2+}]_T$, or $[Mn^{2+}]_T$, and approximating $[M^{2+}]_B$ by $[M^{2+}]_T$ and T^p_{1c} by T^p_{1p} is fully justified (Hamm & Cooperman, 1978).

Water Proton Relaxation Rates (PRR). In previous work, we showed that measurements of ϵ_{obsd} in solutions containing enzyme, Mn^{2+}, and P_i, in which [enzyme]$_T$ > $[Mn^{2+}]_T$, allowed measurement of two dissociation constants, corresponding to P_i binding to sites 1 and 2, as well as of enhancement values for the ternary EMnP and quaternary $EMnP_2$ complexes (Hamm & Cooperman, 1978). In the present work we first extend this approach to examine the interactions of phosphate analogues with EMn. The results are presented in Figure 8.

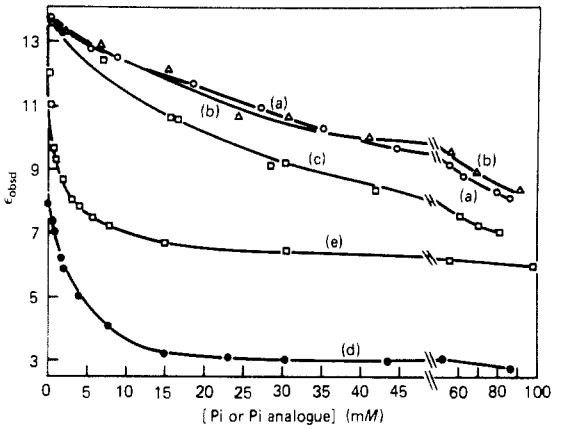

FIGURE 8: Dependence of ϵ_{obsd} on P_i or P_i analogue concentration. All experiments contained 0.10 mM enzyme and 0.04 mM Mn^{2+}. (a) Varying thiophosphate (○); (b) varying phosphoramidate (△); (c) varying methylphosphonate (□); (d) varying methylphosphonate in the presence of 2 mM P_i (●); (e) varying P_i [redrawn from Hamm & Cooperman (1978)] (□).

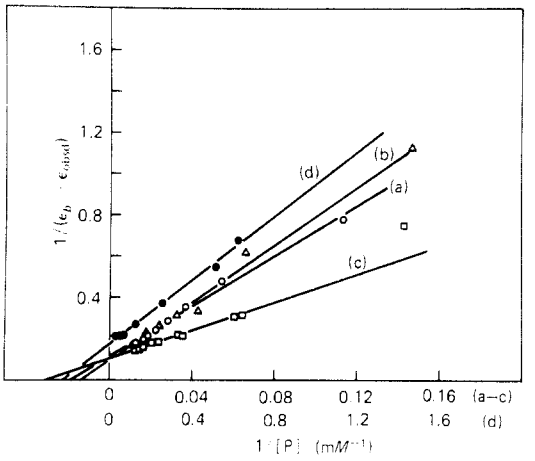

FIGURE 9: Dependence of ϵ_{obsd} on P_i or P_i analogue concentration, plotted according to eq 7. Lines a–d are as described in the legend to Figure 8. Lines drawn are linear least-squares fits to the results.

For all three analogues, only a rather low affinity binding mode is apparent. The simple phenomenological eq 7 adequately

$$\frac{1}{\epsilon_b - \epsilon_{obsd}} = \frac{1}{\epsilon_b - \epsilon_s} + \frac{K_{p,app}}{(\epsilon_b - \epsilon_s)[P]} \quad (7)$$

describes the concentration dependence of ϵ_{obsd}, where ϵ_b is the enhancement of the EMn complex and ϵ_s is the limit of ϵ_{obsd} at saturating $[P]_T$. The reciprocal in Figure 9 allow evaluation of $K_{p,app}$ and ϵ_s. These values are collected in Table IV. For both thiophosphate and phosphoramidate $K_{p,app}$ values are lower limits, since even minor (1–2%) contamination with P_i would give curves similar to those obtained even if neither thiophosphate nor phosphoramidate had any affinity for enzyme–Mn^{2+}. For methylphosphonate, there is no P_i contamination, and the $K_{p,app}$ value of 32 mM is reliable. This value corresponds closely to $K_{p,app}$ measured in the ^{31}P studies described above (Table IV) and presumably reflects binding to site 2. Thus, in contrast with P_i, methylphosphonate binding to site 1 results in little apparent change in ϵ_{obsd}. As can be seen by comparison of curves c and d in Figure 8, the addition of 2 mM P_i considerably enhances EMn affinity for methylphosphonate. We interpret this result as showing that methylphosphonate binds much more strongly to site 2 when P_i replaces methylphosphonate in site 1. Accordingly, for the reciprocal plot d in Figure 9, ϵ_t, the enhancement value for

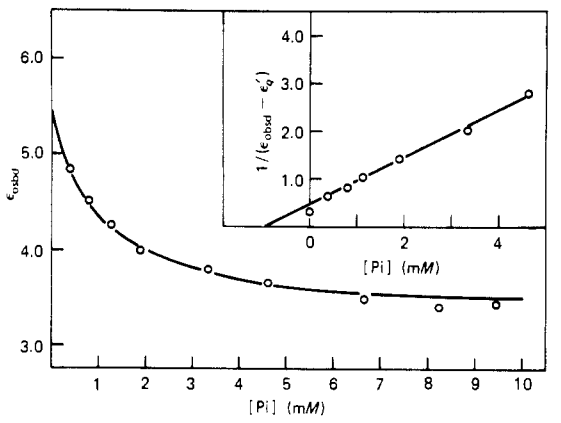

FIGURE 10: Dependence of ϵ_{obsd} on $[P_i]$. $[E]_T$, 0.10 mM, $[Mn^{2+}]_T$, 0.20 mM. (Inset) Plot of data according to eq 5.

Table VI: Water Proton Relaxation Rates

$[E]_T$ (mM)	$[Mn^{2+}]_T$ (mM)	P_i or P_i analogue	$K_{p,app}$ (mM)	ϵ_s or $\epsilon_{complex}$	ref
0.10	0.040	P_i	0.24	7.7 (ϵ_t)	*a*
			14	5.5 (ϵ_q)	*a*
0.10	0.040	CP[c]	32	5.1	*b*
0.10	0.040	CP + 2 mM P_i	4.3	2.1	*b*
0.10	0.040	SP[d]	≥53	5.7	*b*
0.10	0.040	NP[e]	≥72	4.4	*b*
0.10	0.20	P_i	0.95	5.5 ($\epsilon_{t'}$)	*b*
				3.45 ($\epsilon_{q'}$)	*b*

[a] Hamm & Cooperman, 1978. [b] This work. [c] Methylphosphonate. [d] Thiophosphate. [e] Phosphoramidate.

the complex EMnP (equal to 7.7; Hamm & Cooperman, 1978), replaces ϵ_b in eq 7.

The variation of ϵ_{obsd} with P_i was also studied at 2:1 $[Mn^{2+}]/[E]_T$ (Figure 10). When $[P_i]_T \geq 1.0$ mM, essentially all the enzyme in solution contains at least one bound P_i and eq 8 is approximately valid, where ϵ_t' is the average en-

$$\frac{1}{\epsilon_{obsd} - \epsilon_q'} = \frac{1}{\epsilon_t' - \epsilon_q'}\left(\frac{[P_i]}{K_{p,app}} + 1\right) \quad (8)$$

hancement per Mn^{2+} in the complex EMn_2P and ϵ_q' is the average enhancement per Mn^{2+} in the complex EMn_2P_2. The value of ϵ_q' equal to 3.45 was estimated directly from the results shown in Figure 10 as the limiting value of ϵ_{obsd} at saturating $[P_i]$. A plot of $[1/(\epsilon_{obsd} - \epsilon_q')]$ vs. $[P_i]$ gave a straight line (Figure 10, inset) permitting evaluation of $K_{p,app}$ and ϵ_t'. These values are listed in Table VI.

Finally, measurements of ϵ_{obsd} when $[Mn^{2+}]_T > [E]_T$ and $[E]_T$ is large compared to the dissociation constant for P_i binding determined by equilibrium dialysis (Table II) permitted estimation of the stoichiometry of high-affinity P_i binding. This estimate is made from the point of intersection of a line drawn with the initial slope of the ϵ_{obsd} vs. $[P_i]_T$ curve and a line of zero slope drawn as the limiting value of ϵ_{obsd} at saturating inorganic concentration (Figure 11) as determined by a smalll extrapolation of the data to infinite $[P]_T$. For curve a (0.060 mM subunit), the limiting value of ϵ_{obsd} is 1.47 and the point of intersection occurs of 0.060 mM inorganic phosphate, giving a site stoichiometry of 1.00/subunit. For curve b (0.10 mM subunit), the limiting value of ϵ_{obsd} is 1.76 and the point of intersection occurs at 0.085 mM inorganic phosphate, giving a site stoichiometry of 0.85/subunit.

Interpretation of Results and Discussion

This section is divided into four parts. In the first we show how the equilibrium dialysis and ^{31}P NMR data presented in

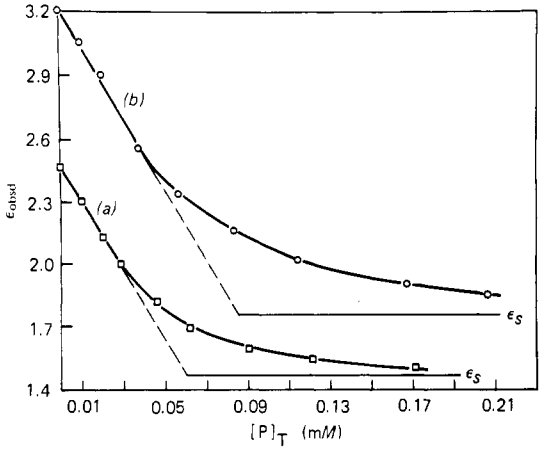

FIGURE 11: Dependence of ϵ_{obsd} on $[P_i]_T$ at fixed $[Mn]_T$ and $[E]_T$. (a) $[E]_T$, 0.060 mM, and $[Mn^{2+}]_T$, 0.60 mM; (b) $[E]_T$, 0.10 mM, and $[Mn^{2+}]_T$, 0.60 mM.

Scheme I: Relevant Equilibria in Solutions of Enzyme, Divalent Metal Ion, and P_i

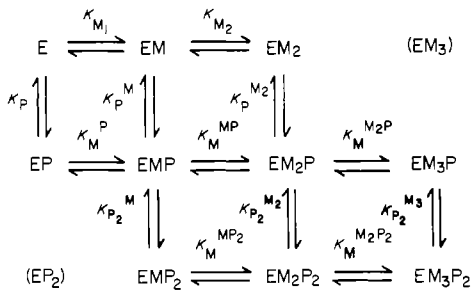

this and an earlier paper (Hamm & Cooperman, 1978) allow us to evaluate all of the important equilibrium constants describing Mn^{2+}, Co^{2+}, and P_i binding to PPase and compare $K_{p,app}$ values predicted by these evaluated constants with those measured by protection of enzymatic activity against inactivation and by a PRR experiment. In the second, we consider the evidence for a conformational change on the enzyme accompanying the binding of a third metal ion. In the third we discuss phosphate and phosphate analogue binding to enzyme and the variation in affinity with the identity of added divalent metal ion. Finally, we conclude with a discussion of what we presently know about the relative locations of P_i and divalent metal ions on the enzyme surface.

Evaluation of Equilibrium Constants. The equilibrium dialysis results presented in Figures 1 and 2 and Table II and the stoichiometric titrations seen in Figures 4 and 11 show clearly the presence of one high-affinity P_i site per enzyme subunit (site 1) and also show that, in addition to the two high-affinity divalent metal ions bound per PPase subunit previously found by Rapoport et al. (1973), a third divalent metal ion binds in the presence of added P_i. The overall enzymatic reaction requires an additional P_i site (site 2), and direct evidence for such a site has been presented by us previously (Hamm & Cooperman, 1978; Springs et al., 1981). Therefore, in solutions of enzyme, Mn^{2+} or Co^{2+}, and P_i we have potentially 12 species to consider, as shown in Scheme I. In fact, in our treatment we consider EM_3 to be stoichiometrically insignificant over the concentration ranges we employ, on the basis of the Scatchard plots for Mn^{2+} and Co^{2+} binding in the absence of P_i (Figure 1). EP_2 is also considered negligible, because of the strong dependence on metal ion of P_i binding to site 2 (see Table VIII), the already weak affinity of P_i for EMP, and the relatively low P_i concentrations employed in the dialysis studies. Finally, we note that the concentration term $[EM_3P_2]_t$ represents the sum of $[EM_3P_2]$ and $[EM_3PP_i]$. Elsewhere, we have shown, at least for Mg^{2+}, that appreciable amounts of EM_3PP_i are formed in equilibrium with EM_3P_2 (Springs et al., 1981), and the studies presented in this paper do not distinguish between these species.

Table VII: Definitions and Equations Used for Estimation of K_P, K_P^M, $K_P^{M_2}$, $K_{P_2}^{M_2}$, $K_M^{M_2P}$, and $K_{P_2}^{M_3}$

$$f = 1 + ([P_i]/K_P^M)(1 + [P_i]/K_{P_2}^M)$$

f_a is the value of f at $[P_i]_a$; f_b is the value of f at $[P_i]_b$

$$A = \frac{K_{M_2,app,b}[P_i]_b}{K_{M_2,app,a}[P_i]_a} \frac{[K_{M_1}f_a(1 + [P_i]_a/K_B) - K_{M_2,app,a}]}{[K_{M_1}f_b(1 + [P_i]_b/K_B) - K_{M_2,app,b}]}$$

$$K_P = \frac{[P_i]}{[fK_{M_1,app}/K_M(1 + [P_i]/K_B)] - 1} \quad (9)$$

$$K_P^M = \frac{K_{M_1,app}(1 + [P_i]/K_{P_2}^M)[P_i]}{K_M[1 + ([P_i]/K_B)(1 + [P_i]/K_P)]} \quad (10)$$

$$K_{P_2}^{M_2} = \frac{A[P_i]_b - [P_i]_a}{1 - A} \quad (11)$$

$$K_P^{M_2} = \frac{K_{M_2,app}[P_i](1 + [P_i]/K_{P_2}^{M_2})}{fK_{M_2}(1 + [P_i]/K_B) - K_{M_2,app}} \quad (12)$$

$$K_M^{M_2P} = \frac{K_{P_1,app}[M]}{K_P^{M_2} - K_{P_1,app}} \quad (13)$$

$$K_{P_2}^{M_3} = \frac{[P_i]K_{M_3,app}}{K_M^{M_2P}(1 + K_P^{M_2}/[P_i] + [P_i]/K_{P_2}^{M_2})(1 + [P_i]/K_B) - K_{M_3,app}} \quad (14)$$

Table VIII: Dissociation Constants

definitions	values (mM) none	Mn^{2+}	Co^{2+}
$K_P = [E][P]/[EP]$	0.80		
$K_B = [M][P]/[MP]$		20	4.6
$K_{M_1} = [E][M]/[EM]$		0.0103	0.0165
$K_{M_2} = [EM][M]/[EM_2]$		0.041	0.066
$K_P^M = [EM][P]/[EMP]$		0.24	0.54
$K_{P_2}^M = [EMP][P]/[EMP_2]$		18	11.5
$K_P^{M_2} = [EM_2][P]/[EM_2P]$		0.25	0.32
$K_{P_2}^{M_2} = [EM_2P][P]/[EM_2P_2]$		0.75	3.8
$K_M^{M_2P} = [EM_2P][M]/[EM_3P]$		0.029	0.21
$K_{P_2}^{M_3} = [EM_3P][P]/[EM_3P_2]_t$		0.66	0.82

There are a total of nine independent equilibrium constants which link the remaining 10 species. For Mn^{2+}, two of these, K_P^M and $K_{P_2}^M$, have been determined by us previously by water proton relaxation rate measurements (Hamm & Cooperman, 1978), and two others, K_{M_1} and K_{M_2}, may be estimated directly from the Scatchard plot of equilibrium dialysis results for Mn^{2+} binding in the absence of P_i (Table II). Further equilibrium dialysis measurements of Mn^{2+} binding to enzyme in the presence of P_i and of P_i binding to enzyme in the presence of Mn^{2+} provide values for $K_{M_1,app}$, $K_{M_2,app}$, $K_{M_3,app}$, and $K_{P,app}$, (Table II) permitting estimation of the five remaining equilibrium constants K_P, $K_P^{M_2}$, $K_{P_2}^{M_2}$, $K_M^{M_2P}$, and $K_{P_2}^{M_3}$ from eq 9 and 11–14 (Table VII). Estimates for all nine constants are presented in Table VIII.

For Co^{2+}, K_{M_1} and K_{M_2} are estimated directly from the Scatchard plot of equilibrium dialysis results for Co^{2+} binding in the absence of P_i (Table II), and $K_{P_2}^M$ and $K_{P_2}^{M_2}$ are estimated directly from the concentration dependence of the ^{31}P longitudinal relaxation rates (Table IV). With K_P already estimated from the results with Mn^{2+}, the remaining four

Table IX: Comparison of Predicted and Experimental $K_{p,app}$ (mM) Values

expt. no.	method	$[E]_T$ (mM)	$[M^{2+}]_T$ (mM)	predicted $K_{p_1,app}$	predicted $K_{p_2,app}$	measured $K_{p,app}$
1	PhGx protection	0.0023	Mn^{2+}, 1.0	0.0070	0.66	0.0094
2	PhGx protection	0.028	Co^{2+}, 1.0	0.056	0.82	0.090
3	EDAC protection	0.0095	Co^{2+}, 1.0	0.056	0.82	0.058
4	water PRR	0.10	Mn^{2+}, 0.20	0.24	1.59	0.95
5	PhGx protection	0.028	Mg^{2+}, 10	0.52	27	2.4
6	EDAC protection	0.025	Mg^{2+}, 10	0.52	27	4.5

constants, K_P^M, $K_P^{M_2}$, $K_M^{M_2P}$, and $K_{P_2}^{M_3}$, can be estimated from measured $K_{M_1,app}$, $K_{M_2,app}$, $K_{M_3,app}$, and $K_{P_1,app}$ values (Table II) and eq 10 and 12–14 (note that eq 10 is just a rearranged version of eq 9). Estimates for these constants are also presented in Table VIII.

The values in Table VIII enable us to predict K_{app} values for P_i sites 1 and 2 at given values of P_i and Mn^{2+} or Co^{2+} concentrations. In Table IX such predicted values are compared with $K_{P,app}$ values measured under conditions similar to (for the protection against inactivation of enzymatic activity experiments) or identical with (for the PRR experiment) those used in determining the values given in Table VIII. Also compared in Table IX are $K_{P_1,app}$ and $K_{P_2,app}$ values determined in the presence of Mg^{2+} from an analysis of the dependence of enzyme-bound PP_i formation on P_i concentration (Springs et al., 1981) with $K_{P,app}$ values measured in the PhGx and EDAC protection experiments.

The K_{app} from the PRR experiment, performed in the presence of Mn^{2+}, agrees fairly well with the predicted value for $K_{P_2,app}$. This is an important consistency check for our analysis, since it represents a direct determination of what is essentially $K_{P_2}^{M_2}$ in the presence of Mn^{2+}, a constant which we had otherwise evaluated only indirectly from eq 11. For the PhGx protection experiments in the presence of Mn^{2+} or Co^{2+}, the closeness of agreement between $K_{P,app}$ and the predicted $K_{P_1,app}$ values provides strong evidence that it is P_i binding to site 1 alone that results in protection of an essential arginine (Bond et al., 1980) which we elsewhere have shown to be Arg-77. Given the known ability of arginine to hydrogen bond to P_i (Cotton et al., 1974), it would be reasonable to attribute the observed protection to the direct interaction of P_i in site 1 with Arg-77.

Evidence for a Conformational Change. Although Arg-77–Pi (site 1) hydrogen bonding may indeed by necessary for protection, other results lead us to suggest that maximal protection requires, in addition, a conformational change accompanying the binding of a third divalent metal ion, which makes the enzyme active site less accessible to solvent. The evidence for this suggestion is 3-fold. First, there is the direct experiment presented in Figure 5, showing that although P_i binds to PPase in the absence of added divalent metal ion and confers partial protection, maximal protection requires three enzyme-bound Mn^{2+}. Second, the value of $K_{P,app}$ measured in the presence of Mg^{2+} by protection against PhGx inactivation falls in between the $K_{P_1,app}$ and $K_{P_2,app}$ values found in measurements of enzyme-bound PP_i formation, even allowing for small differences which could arise from differences in the reaction media for the two experiments. We interpret these results as showing that, in the presence of Mg^{2+}, the binding of a single P_i affords only partial protection, with full protection requiring the binding of both phosphates per subunit. This is consistent with our suggestion, since unlike the binding of a third Co^{2+} or Mn^{2+}, which requires the binding of only a single phosphate per subunit, the binding of a third Mg^{2+} to the enzyme (at 10 mM $[Mg^{2+}]$) requires the binding of two phosphates per subunit (Springs et al., 1981). Third, the average value per Mn^{2+} of the PRR enhancement parameter progressively decreases for the complexes $EMnP_i$, EMn_2P_i, and EMn_3P_i, having the value 7.7 for $EMnP_i$ (Hamm & Cooperman, 1978), 5.5 for EMn_2P_i (Table V), and 2.4 for EMn_3P_i (as estimated from the plateau values in Figure 11). This trend supports our suggestion, since ϵ provides a measure of the accessibility of solvent water to enzyme-bound Mn^{2+}. It might be argued that the fact that $K_{P,app}$ values measured by protection against EDAC inactivation are similar to or identical with those measured by protection against PhGx inactivation provides a fourth piece of evidence for a conformational change restricting solvent access to the active site, since charge repulsion should prevent the carboxylate side chains that are the most likely targets of EDAC modification from interacting directly with P_i. However, this result could also reflect direct metal ion interaction with these side chains, since, under the conditions of our experiments, the binding of the third divalent metal ion occurs concurrently with phosphate binding (Figure 1).

Phosphate and Phosphate Analogue Binding. Phosphate affinity for site 1 varies considerably as a function of the identity of added divalent metal ion, a result which we can, as a result of our analysis of divalent metal ion and P_i binding, attribute directly to differences in the binding of the third divalent metal ion and more specifically to differences in the value of $K_M^{M_2P}$. Thus $K_{P_1,app}$ is 0.009–0.014 mM in the presence of Mn^{2+} (0.5–1.0 mM), 0.06–0.09 mM in the presence of Co^{2+} (1.0 mM), 0.11 mM in the presence of Zn^{2+} (assuming that, as with Mn^{2+} and Co^{2+}, P_i binding in site 1 protects against PhGx inactivation), and 0.5 mM in the presence of 10 mM Mg^{2+}, and $K_M^{M_2P}$ follows the same trend, 0.029 mM for Mn^{2+}, 0.22 mM for Co^{2+} (Table VIII), and >10 mM for Mg^{2+} (Springs et al., 1981). By contrast, the values of K_P^M for Mn^{2+} and Co^{2+} and of $K_P^{M_2}$ for Mn^{2+}, Co^{2+}, or Mg^{2+} (same as $K_{P_1,app}$ at 10 mM Mg^{2+}) differ little from each other or from K_P (Table VIII). Phosphate affinity for site 2 also varies as a function of divalent metal ion, being considerably less in the presence of Mg^{2+} than in the presence of either Co^{2+} or Mn^{2+} (Table IX). The effect of divalent metal ion on relative P_i affinity thus shows an inverse correlation with the effectiveness of divalent metal ion as a cofactor for catalytic enzyme activity, which for both PP_i hydrolysis and water–P_i oxygen exchange falls in the order $Mg^{2+} > Zn^{2+} > Co^{2+} \approx Mn^{2+}$ (Janson et al., 1979; Butler & Sperow, 1977). This is perhaps not surprising since higher affinity is consistent with a slower dissociation rate, and elsewhere we (Springs et al., 1981) and others (Hackney & Boyer 1978; Cohn & Hu, 1978; Hackney, 1980) have shown that release of each P_i from enzyme is partially rate determining in overall enzyme-catalyzed PP_i hydrolysis.

Studies of P_i analogue binding to PPase were undertaken in order to provide information on the structural requirements of sites 1 and 2. PRR and ^{31}P studies show that both phosphoramidate and thiophosphate have lower affinity for PPase

than P_i. Since interpretation of experiments with these analogues would be complicated by the presence of even minor contaminating amounts of P_i, we have concentrated our efforts on methylphosphonate, where such contamination is not a problem.

Our results indicate that methylphosphonate is a much poorer ligand than P_i for site 1 but is comparable as a ligand for site 2. Thus, when $[Mn^{2+}]_T < [E]_T$, the apparent dissociation constants for site 1 are 0.24 mM for P_i and 6.7 mM for methylphosphonate (Tables IV and VI). Similarly, when $[Mn^{2+}]_T > [E]_T$, the apparent site 1 dissociation constants measured by protection against PhGx inactivation are 0.0097 mM for P_i and 4.1 mM for methylphosphonate (Table III). This large difference in affinity may be due at least in part to an inability of the enzyme to undergo the putative conformational change reducing active site accessibility to solvent when methylphosphonate replaces P_i. This possibility is suggested by the result that the protection against PhGx inactivation afforded by saturating methylphosphonate is much less than that afforded by saturating P_i. On the other hand, the apparent dissociation constants for site 2 when $[Mn^{2+}]_T < [E]_T$ are similar: 14–18 mM for P_i and 32–35 mM for methylphosphonate (Table IV and VI). Moreover, in the presence of 2 mM P_i, which is sufficient to almost saturate site 1 while site 2 remains essentially open, the apparent dissociation constant for methylphosphonate, which should measure binding to the low-affinity site, is 4.3 mM, that is, considerably lower than the value of 14–18 mM for P_i itself.

Metal Ion to P_i Distances on PPase. In this and previous work (Hamm & Cooperman, 1978; Springs et al., 1981), we have demonstrated the presence, per PPase subunit, of two sites for P_i binding of different affinities and specificities and shown that the high-affinity site 1 contains an essential arginine. We also have shown that three divalent metal ions bind per enzyme subunit, and are necessary for enzymatic activity, and presented evidence for a conformational change accompanying the binding of a third divalent metal ion. It now remains to ascertain the functional roles of these metal ions in the catalytic process. A first goal, which has thus far only been partially achieved, is the determination of the distances between the bound divalent metal ions and P_i in sites 1 and 2, and it is with a discussion of our current knowledge on this point that we will conclude this paper.

Previously, we used the measured effect of enzyme containing one Mn^{2+} per subunit on the T_1 of enzyme-bound P_i to calculate a $Mn^{2+}/^{31}P$ distance of 6.2 ± 0.4 Å, consistent with a second sphere complex between the enzyme-bound Mn^{2+} and P_i in site 2 (Hamm & Cooperman, 1978). In view of our current results showing that in the presence of P_i, the intrinsic binding constants for all three Mn^{2+} which can be bound are roughly equivalent, this distance is actually a weighted root mean sixth average for metal ion bound in all three potential sites. This raises the possibility that one divalent metal ion site, occupied only partially, is responsible for all of the observed relaxation and thus is considerably closer to P_i than 6.2 Å. On the basis of the near equivalency of divalent metal ion site affinities, it is reasonable to assume that no one of the three sites contains <10% of enzyme-bound metal ion. However, even the extreme assumption that only 10% of the enzyme-bound Mn^{2+} is responsible for all of the observed ^{31}P relaxation would lead to a calculated Mn–P_i (site 2) distance of 4.2 Å, which is considerably greater than the inner sphere distance of 2.7–2.9 Å (Mildvan & Grisham, 1974) expected for an Mn–P_i complex. We therefore conclude that in the $EMnP_2$ complex, none of the three possible Mn^{2+} sites are close enough for direct binding to P_i in site 2. However, because of our evidence for a conformational change accompanying the binding of a third divalent metal ion, this conclusion does not rule out inner sphere Mn^{2+}–P_i (site 2) binding in the catalytically active (Springs et al., 1981) EMn_3P_2 complex.

In our earlier study (Hamm & Cooperman, 1978) we could detect no relaxation by enzyme-bound Mn^{2+} of P_i in site 1 and were unable to decide whether this lack of observed effect indicated a rather large distance between enzyme-bound Mn^{2+} and P_i in site 1 or was due rather to slow chemical exchange of P_i in site 1 with P_i in solution. The latter interpretation would require a mean residence time of P_i in site 1 of >7 ms.

In the present study, measurements of the effect of enzyme-bound Co^{2+} on the $T_{1p}^{\P}$ were used principally to estimate $K_{P_2}^{M}$ and $K_{P_2}^{M_2}$ and are incomplete with respect to calculation of Co^{2+}–P_i distances. Nevertheless, they do allow some conclusions to be drawn. First, we see no evidence for Co^{2+} interaction with P_i in site 1 in the complex ECoP, which would have shown up as a negative deviation from line a in Figure 7 at low P_i concentration (line b, at a Co^{2+}/enzyme subunit ratio of 1.8:1.0, was not extended to low enough concentration to test for such a deviation). We estimate that a mean residence time of P_i in site 1 > 50 ms would be required for this lack of observed effect to result from slow chemical exchange. Given the value for K_P^M of 0.54 mM (Table VIII), this in turn would require a second-order binding constant of P_i to ECo of 3×10^4 M^{-1} s^{-1}, which is extremely slow for simple P_i binding to a protein. This result strengthens the argument that in an enzyme subunit containing one bound divalent metal ion, the divalent metal ion is not close to site 1. Second, the $T_{1q}^{\P}$ and $T_{1q'}^{\P}$ values measured respectively for $ECoP_2$ and ECo_2P_2 (Table V) allow calculation of lower limits for the root mean sixth Co^{2+}–P_i (site 2) distance, r, on the basis of the assumption that of the four mechanisms which can contribute to ^{31}P relaxation [diamagnetic relaxation, outer sphere relaxation, dipolar interaction, and hyperfine contact (Mildvan & Gupta, 1979)] only dipolar interaction is important. Thus r is given by inequality 15, where ω_I and ω_s are the nuclear and electronic

$$r \geq (658 \pm 132)\left[T_{1,\text{complex}}^{\P}\left(\frac{3\tau_c}{1+\omega_I^2\tau_c^2}+\frac{7\tau_c}{1+\omega_s^2\tau_c^2}\right)\right] \quad (15)$$

precession frequencies, respectively, τ_c is the correlation time for the dipolar interaction, and 658 ± 132 is the numerical value of a constant term for Co^{2+}–^{31}P interaction (Mildvan & Gupta, 1979). The Co^{2+} complexes of enzyme are pink, characteristic of high-spin Co^{2+}. For example, for the ECo_2P complex the relevant spectral parameters are as follows: λ_{max} (nm) 460, 492, 550 (ϵ 14, 14, 8). The electron spin relaxation time of high-spin Co^{2+}, which should dominate τ_c, ranges from 5×10^{-13} to 10^{-11} s. The value of $T_{1q}^{\P}$ for $ECoP_2$, 0.0088 s (Table V), thus gives a value for $r \geq 3.9$–5.4 Å, where ≥3.9 Å corresponds to a τ_c of 5×10^{-13} s and ≥5.4 Å to a τ_c of 10^{-11} s. The value of $T_{1q}^{\P}$ for ECo_2P_2 is 0.0038 s (Table V). If both Co^{2+} ions are assumed to interact equally with P_i in site 2, then from inequality 15, $r \geq 3.8$–5.2 Å; if only one Co^{2+} interacts, then $r \geq 3.4$–4.7 Å. As these estimates make clear, it will be of obvious value to extend our measurements to the ECo_3P_2 complex and to evaluate both τ_c and the magnitude of the dipolar contribution to ^{31}P relaxation in order to calculate r more accurately. Such measurements are currently under way.

Acknowledgments

We acknowledge the assistance of Ben Kruskal, who helped

with some of the experiments described above.

References

Åkerfeldt, S. (1960) *Acta Chem. Scand. 14*, 1980–1984.
Bond, M. W. (1979) Ph.D. Thesis, University of Pennsylvania, Philadelphia, PA.
Bond, M. W., Chiu, N. Y., & Cooperman, B. S. (1980) *Biochemistry 19*, 94–102.
Butler, L. G., & Sperow, J. W. (1977) *Bioinorg. Chem. 7*, 141–150.
Chambers, R. W., & Khorana, H. G. (1958) *J. Am. Chem. Soc. 80*, 3749–3752.
Cohn, M., & Leigh, J. S. (1962) *Nature (London) 193*, 1037–1040.
Cohn, M., & Hu, A. (1978) *Proc. Natl. Acad. Sci. U.S.A. 75*, 200–203.
Cooperman, B. S., & Chiu, N. Y. (1973a) *Biochemistry 12*, 1670–1675.
Cooperman, B. S., & Chiu, N. Y. (1973b) *Biochemistry 12*, 1676–1682.
Cooperman, B. S., Chiu, N.Y., Bruckmann, R. H., Bunick, G. J., & McKenna, G. P. (1973) *Biochemistry 12*, 1665–1669.
Cotton, F. A., Day, V. W., Hazen, E. E., Jr., Larsen, S., & Wong, S. T. K. (1974) *J. Am. Chem. Soc. 96*, 4471–4478.
Eisinger, J., Shulman, R. G., & Szymanski, B. M. (1962) *J. Chem. Phys. 36*, 1721–1729.
Hackney, D. D. (1980) *J. Biol. Chem. 255*, 5320–5328.
Hackney, D. D., & Boyer, P. D. (1978) *Proc. Natl. Acad. Sci. U.S.A. 75*, 3133–3137.
Hamm, D. J., & Cooperman, B. S. (1978) *Biochemistry 17*, 4033–4040.
Janson, C. A., Degani, C., & Boyer, P. D. (1979) *J. Biol. Chem. 254*, 3743–3749.
Klement, R., & Becht, K. H. (1947) *Z. Anorg. Chem. 254*, 217–220.
Kunitz, M. (1952) *J. Gen. Physiol. 35*, 423–450.
Lietzke, M. H. (1963) *A Generalized Least-Squares Program for the IBM 7090 Computer*, DRNL-3295, Office of Technical Service, U.S. Department of Commerce, Washington, DC.
Mildvan, A. S., & Grisham, C. M. (1974) *Struct. Bonding (Berlin) 20*, 1–21.
Mildvan, A. S., & Gupta, R. K. (1979) *Methods Enzymol. 49*, 322–359.
Navon, G., Shulman, R. G., Wyluda, B. G., & Yamane, T. (1970) *J. Mol. Biol. 51*, 15–30.
Rapoport, T. A., Höhne, W. E., Heitmann, P., & Rapoport, S. (1973) *Eur. J. Biochem. 33*, 341–347.
Scatchard, G. (1949) *Ann. N.Y. Acad. Sci. 51*, 660–672.
Schaffner, W., & Weissmann, C. (1973) *Anal. Biochem. 56*, 502–514.
Springs, B., Welsh, K. M., & Cooperman, B. S. (1981) *Biochemistry* (in press).
West, T. S. (1969) *Complexometry*, B. D. H. Chemical Ltd., Poole, England.

Use of Phospholipase D To Alter the Surface Charge of Membranes and Its Effect on the Enzymatic Activity of D-β-Hydroxybutyrate Dehydrogenase†

Robert M. Clancy, Alan R. Wissenberg, and Michael Glaser*

ABSTRACT: The effect of an electrostatic potential on the enzymatic activity of D-β-hydroxybutyrate dehydrogenase was examined. Phospholipase D was used to increase the surface charge and concomitantly the electrostatic potential of submitochondrial membranes. The apparent K_m for the negatively charged substrates of D-β-hydroxybutyrate dehydrogenase increased as the membranes were reacted with phospholipase D. There was a 10-fold increase in the apparent K_m for NADH when the content of acidic phospholipids was increased by 24%. The addition of monovalent or divalent cations, which reduced the electrostatic potential, largely reversed the apparent K_m changes. At the same ionic strength, divalent cations had a substantially larger effect than monovalent cations. Similar results were obtained when the purified apoenzyme was reconstituted in unilamellar vesicles containing different ratios of phosphatidylcholine and acidic phospholipids. When the apoenzme was reconstituted into phosphatidylcholine vesicles containing increasing amounts of phosphatidylethanolamine, the apparent K_m also increased but to a smaller extent, and increasing the ionic strength did not reverse this effect. The results show that the apparent K_m of D-β-hydroxybutyrate dehydrogenase can be significantly altered by an electrostatic potential as well as other properties of the phospholipid polar head group.

Electrostatic potentials have been shown to affect the catalytic activity of enzymes in a variety of systems (Douzou & Maurel, 1977). One approach to studying these effects has been to immobilize trypsin and chymotrypsin to an insoluble polyanionic carrier (Goldstein et al., 1964; Goldstein, 1972). The polyanionic environment was found to promote a strong local negative electrostatic potential which acted on the chemical properties of the medium. In particular, the local concentration of ionic species were found to be different from those of the bulk solution. Another study employing lysozyme in the polyanionic environment of the cell wall of *Micrococcus luteus* has shown similar results (Maurel & Douzou, 1976). Relatively few studies have been carried out on the effect of an electrostatic potential on the properties of membrane-bound enzymes. Recently, Wojtczak & Nalecz (1979) and Nalecz et al. (1980) used detergent methods and fatty acids to increase the electrostatic potential of a biological membrane and observed the effect on several membrane-bound enzymes.

† From the Department of Biochemistry, University of Illinois, Urbana, Illinois 61801. *Received April 16, 1981.* This work was supported by National Institutes of Health Grant GM 21953. M.G. was supported by National Institutes of Health Research Career Development Award GM 00193.

0006-2960/81/0420-6060$01.25/0